Article

Behaviour and Design of Bolt-Coupler Connections under Compression in Prefabricated CFST Columns

Md Kamrul Hassan *[iD], Bulbul Ahmed [iD], Anmol Ram and Swapan Saha

School of Engineering, Design and Built Environment, Western Sydney University, Penrith, NSW 2751, Australia
* Correspondence: k.hassan@westernsydney.edu.au

Abstract: The paper presents the investigated results of bolt-coupler connections under compression experimentally. Bolt-coupler connections have been developed recently for prefabricated column-to-column (PCC) connections to simplify the construction process of prefabricated concrete-filled steel tubular (CFST) columns and to transfer the upper column load to the bottom column through bolt-coupler connections. However, the behaviour of bolt-coupler connections under compression has not been investigated in the past although there are some experimental and numerical studies conducted on bolt-coupler connections under tension. To address these research gaps, the behaviour of bolt-coupler connections under compression has been investigated. The main parameters considered in this study are bolt diameters (M16, M20, M24), bolt grades (8.8, 10.9 grade), gap inside the coupler between two bolts of bolt-coupler connection (0, 10, 20 mm), and coupler grade (5.6, 8.8 grade). It is observed that the ultimate capacity of bolt-coupler connections is reduced significantly with an increase in the bolt gap inside the coupler of the bolt-coupler connection. Based on the test data, a design equation is developed to determine the design capacity of bolt-coupler connections under compression, which will be very useful in designing the PCC connections of sustainable prefabricated CFST columns.

Keywords: structural bolts; couplers; bolt-coupler connections; prefabricated column connections; compression behaviour

1. Introduction

Prefabricated construction using composite structures is an advanced off-site construction technology and has widely been used in the recent construction industry [1,2]. In this method, the building components are manufactured separately in the industry and assembled on the construction site, which increased sustainability with less construction waste and energy consumption [2–6]. Prefabrication construction is well accepted nowadays due to its constructional, financial, and environmental benefits [3,5]. The structural behaviour significantly improves and allows the structures to consume less energy and materials. Concrete-filled steel tubular (CFST) columns have been widely used in recent prefabrication construction instead of reinforced concrete (RC) or steel columns [2,7,8]. Prefabrication construction using CFST columns has more benefits in terms of structural behaviour, fire resistance, construction cost, and ease of construction compared to conventional RC and steel columns [2,7,9,10]. Although CFST columns are more advantageous in prefabrication construction, the column-to-column connection is the main concern and has been paid more attention to the researchers. To connect two CFST columns, blind bolts have been used in conventional on-site constructions and demountable constructions [11–15]. The applicability of blind bolts in the prefabricated CFST column-to-column connection is quite complicated due to its complex geometry and installation process [2]. Moreover, the developed system is not cost-effective as the blind bolts are highly expensive compared to conventional structural bolts.

To address the existing difficulties and sustainable development in prefabrication, innovative bolt-coupler column-to-column connections had been developed by Hassan et al. [2] to connect one prefabricated CFST column to another prefabricated CFST column. In their proposed connection, Hassan et al. [2] used normal structural bolts instead of blind bolts to reduce the material cost of connection, which can simplify the construction process of two prefabricated CFST columns. Bolt-coupler connections were also used by Yang et al. [16] to connect slabs with steel beams for demountable constructions. The load transfer mechanism of bolt-coupler connections used in prefabricated CFTS columns is totally different when compared to the load transfer mechanism of bolt-coupler connections used in beam-slab connections. In beam-slab connections, bolt-coupler connections are subjected to shear force mainly whereas bolt-coupler connections used in prefabricated CFST columns are under compression [2]. Although Hassan et al. [2] used bolt-coupler connection in prefabricated CFST column-to-column connection and investigated numerically, still there is no evidence of structural behaviour of bolt-coupler connection under compression separately. From the literature, there is no scientific evidence either experimentally or numerically on the bolt-coupler connection under compression, although there is plenty of research on bolt-coupler connection and blind bolted connection under tension [17,18], shear [16,19,20], and combined tension and shear [21,22].

Currently, Yang et al. [16] conducted research on the shear performance of bolt-coupler connection and proposed a novel steel-concrete bolt-coupler connection system for the countability of concrete slabs was determined successfully in terms of push-out test analysis. An embedded bolt-coupler system was used by Nijgh et al. [23] instead of welded-headed studs in steel-concrete composite beams. Xue et al. [20,24] evaluated the most popular Piekko couplers on precast shear walls and beam-column connections under axial compression and seismic action. Concrete with threaded-bolt (CTB) columns was investigated by Qing et al. [17], who developed a simplified model for the ultimate drift ratios of CTB columns. Kumar et al. [18] performed an axial loading test of a threaded coupler system to evaluate the load transfer mechanism and a novel threaded coupler system was proposed for the dual-height rock bolts. Ataei et al. [25] conducted push-out tests on high-strength friction-grip (HSFG) bolts and reported that the HSFG bolts showed brittle behaviour and cannot reach desired slip capacity as Euro code (EN4) defined [26]. Later, blind bolts with a coupler were tested and simulated under static pushout tests by Yang et al. [16,27] and concluded that this bolting system only can achieve ductile behaviour when the diameter of the bolt is 27 mm or larger. The tolerance phenomena were also addressed for the resin-injected bolts with couplers and found satisfactory results for the car park buildings [23].

Furthermore, both experimental and numerical investigation has been performed for high-strength bolted spherical joints (HSBSJ) under tension. A total of 40 tests with different screwing depths were performed and found that the HSBSJ experienced bolt fracture failure, thread failure, and sphere rupture failure [28]. Additionally, the shear behaviour of bolted connection in the prefabricated composite beam was investigated under the push-out test [29,30]. In the research, they proposed a design formula based on the experimental and numerical results for high-strength bolt connections considering bolt pretension, the bolt diameter, the bolt tensile strength and the compressive strength of concrete. As the PCC connection in the prefabricated CFST column is under compression and may not be similar to the behaviour of structural bolts under tension, shear and combined shear and tension, the behaviour of PCC in the proposed design is critical and need to be carefully investigated prior to the application of Hassan et al. [2] column-to-column connection. During tightening the bolts and couplers in the prefabricated CFST column connection, there is a gap inside the coupler. The effect of this gap has not been investigated yet. This bolt spacing gap could impact significantly the compression capacity of the bolt-coupler connection. In addition, there is no design equation to determine the compression capacity of the bolt-coupler connection considering this gap inside of the coupler.

From the literature review, it can be seen that most of the previous research works have been conducted on demountable blind bolts and bolt-coupler connections and were

mainly focused on structural behaviour under tension, shear, and combined tension and shear. Bolt-coupler connection under pure axial compression is still short of a strong scientific basis, which hinders the application of bolt-coupler connections to develop sustainable prefabricated CFST columns. In addition, the failure modes and strength of bolt-coupler connection under compression could be different from tension, shear, and combined tension and shear connection. Consequently, it is worth noting that the existing design codes could be conservative to calculate the strength capacity of bolt-coupler connection under pure axial compression. Based on the above discussion, it is obvious to conduct further research on the bolt-coupler connection under compression. In the present study, an experimental investigation has been carried out to understand the bolt-coupler connections under compression. The diameter of bolts and coupler is selected as 16 mm (M16), 20 mm (M20), and 24 mm (M24) and three different bolt and coupler grades (5.6, 8.8, and 10.9) to assess the eligibility of the bolt-coupler mechanism in Hassan et al. [2] design of prefabricated CFST column-column connections. Moreover, based on the test and numerical data, a design formula for bolt-coupler connections is proposed in this study.

2. Experimental Investigation

2.1. Test Specimens Designed Concept

The innovative PCC connections designed by Hassan et al. [2] using baseplate, bolts, and couplers are proposed to connect two prefabricated CFST columns, as shown in Figure 1a. Two baseplates attached to the top and bottom columns are connected by structural bolts, as shown in Figure 1b. Couplers are used to connect upper bolts with lower bolts to transfer the corner load of the top column to the bottom column through a bolt-coupler connection, as shown in Figure 1c. The upper bolt head is subjected to compression force coming from the corner part of the top column, and the lower bolt head is embedded into the concrete of the bottom CFST column. It can be seen that the bottom surface of the lower bolt head is supported by concrete. To reflect these top and bottom end conditions, the compressive load is applied at the top of the upper bolt head and support is considered at the bottom of the lower bolt head, as shown in Figure 1d. During tightening the bolts and couplers, there is a gap between the upper bolt and lower bolt inside the coupler, as shown in Figure 1c. There could even be a gap between the coupler and nut used to connect two base plates. Based on this assumption, test specimens were designed without considering the nut beneath the coupler. To understand the effect of spacing gaps on the ultimate load of bolt-coupler connections under compression, three different gaps (0, 10, 20 mm) are considered in the experimental study, as shown in Figure 2.
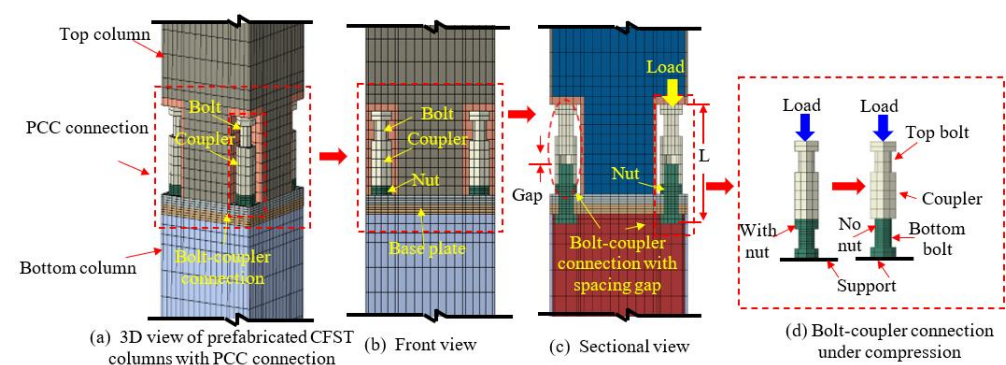

Figure 1. Bolt-coupler connections under compression in prefabricated CFST column.

(a) No spacing gap in between two bolts connected using a coupler

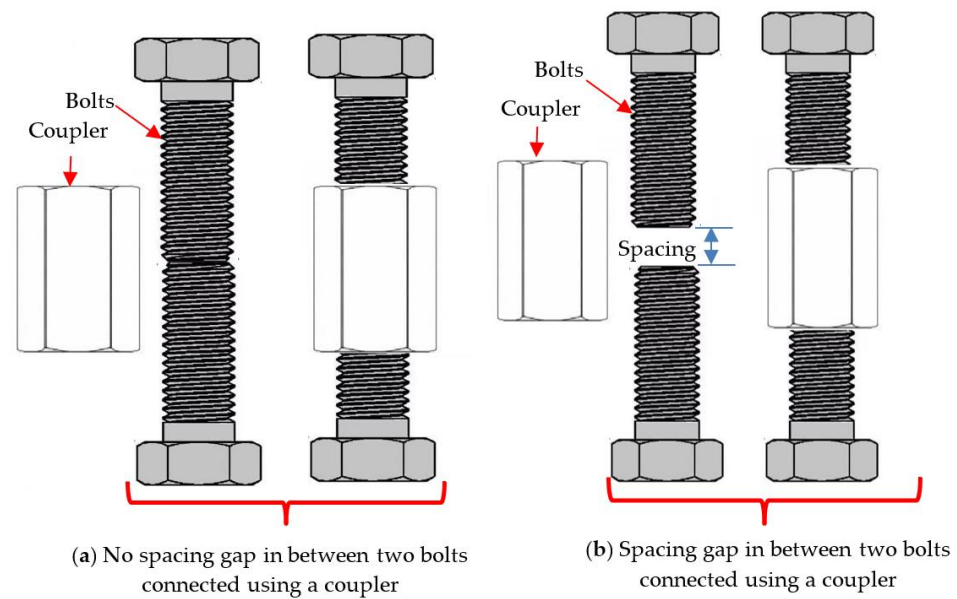(b) Spacing gap in between two bolts connected using a coupler

Figure 2. Bolt-coupler connections with and without spacing gaps.

2.2. Test Specimens

A total of 20 bolt-coupler connection specimens were designed for testing. It is worth mentioning that the repeatability test on bolt-coupler connections under compression was not conducted in this research as bolts and couplers are homogeneous materials. The main parameters considered in this experimental study were bolt diameters (16 mm, 20 mm, and 24 mm), bolt grade (8.8 and 10.9 grade), coupler grade (5.6 and 8.8 grade), and gaps (0, 10, and 20 mm). All bolts and couplers designed according to ISO (ISO898) standard were collected from the local market and used for the test specimens. The bolt-coupler connection specimens were labelled as C-M-BG-CG-X. The identity of specimens refers to: (i) C represents compression loading; (ii) M refers to bolt diameter; (iii) BG indicates bolt grade; (iv) CG indicates the coupler grade, and (v) X refers to face to face distance between upper and lower bolts within the coupler. For instance, the specimen "C-24-8.8-5.6-10" represents the 8.8 grade 24 mm diameter (M24) structural bolt coupling with a 5.6 grade coupler and the face-to-face distance between the top and bottom bolts within the coupler is 10 mm. The geometry and configuration of structural bolts and couplers are depicted in Figure 3.

(a) M16 grade 8.8 bolt   (e) M20 grade 8.8 bolt

(i) M24 grade 8.8 bolt

(b) M16 grade 10.9 bolt   (f) M20 grade 10.9 bolt

(j) M24 grade 10.9 bolt

(g) M20 grade 5.6 coupler

(c) M16 grade 5.6 coupler

(k) M24 grade 5.6 coupler

(d) M16 grade 8.8 coupler   (h) M20 grade 8.8 coupler
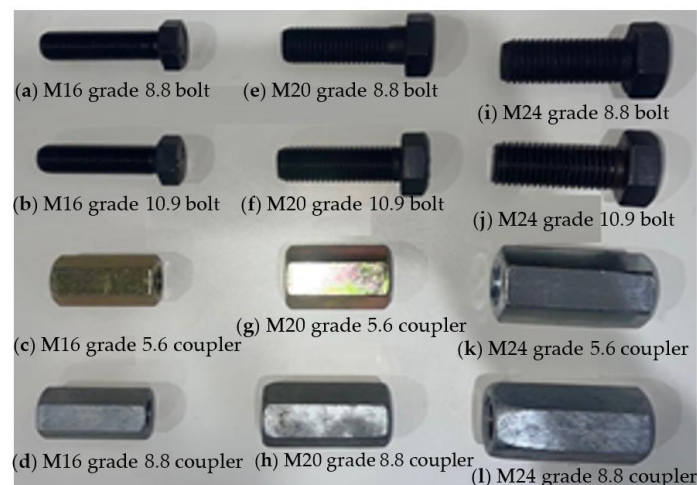
(l) M24 grade 8.8 coupler

Figure 3. Types of bolts and couplers used in this study.

The dimensions of bolts and couplers were measured using a Vernier Caliper and reported the value of (a) thread outer diameter (*D1*); (b) thread inner diameter (*D2*); (c) bolt/coupler length (*L*); (d) thickness of bolt head (*C*); (e) thickness of bolt head (*H*); and (f) bolt head size (*F*) in Tables 1 and 2 and in Figures 4 and 5. Both structural bolts and couplers have the same thread angle 60-degree. For the same-diameter bolts and couplers, the pitch value is similar, and it depends on the bolt/coupler size [31]. The standard value of pitch is 2.0 mm, 2.5 mm, and 3.0 mm for M16, M20, and M24 bolts and couplers, respectively.

Table 1. Geometric properties of structural bolts.

Bolt Type and Grade	*D* (mm)	*D1* (mm)	*D2* (mm)	*H* (mm)	*C* (mm)	*F* (mm)	*L* (mm)	Pitch, *P* (mm)	Thread Angle (°)
M16-8.8	16	15.84	13.84	10.07	27.20	23.81	60.08	2.00	60
M16-10.9	16	15.86	13.86	10.18	27.26	23.83	59.91	2.00	60
M20-8.8	20	19.82	17.30	12.47	34.12	29.91	60.02	2.50	60
M20-10.9	20	19.82	17.26	12.48	34.21	29.92	60.02	2.50	60
M24-8.8	24	23.76	20.72	15.12	40.93	35.63	59.76	3.00	60
M24-10.9	24	23.74	20.74	15.24	40.83	35.61	59.43	3.00	60

Table 2. Geometric properties of structural couplers.

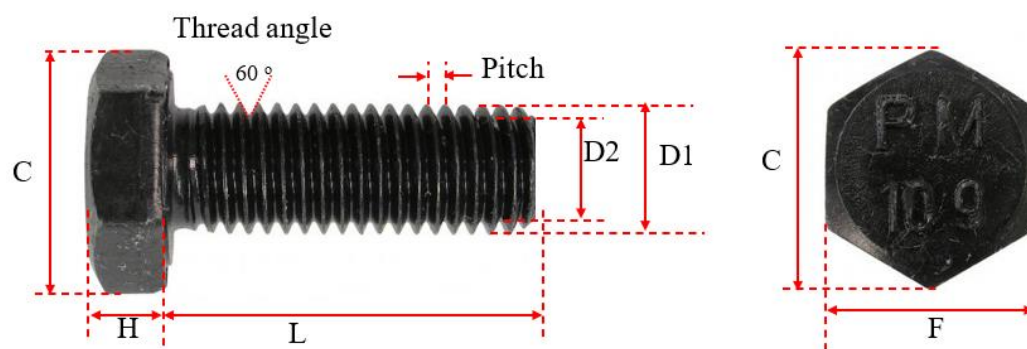| Coupler Type and Grade	*D* (mm)	*D1* (mm)	*D2* (mm)	*C* (mm)	*F* (mm)	*L* (mm)	Pitch (mm)	Thread Angle (°)
M16-8.8	16	15.84	14.78	27.46	23.98	51.92	2.00	60
M16-5.6	16	15.86	14.18	27.34	23.94	49.98	2.00	60
M20-8.8	20	19.82	18.34	33.94	29.84	60.16	2.50	60
M20-5.6	20	19.82	17.84	34.18	29.82	49.71	2.50	60
M24-8.8	24	23.76	21.60	40.30	35.36	71.48	3.00	60
M24-5.6	24	23.74	21.52	40.60	35.48	71.65	3.00	60

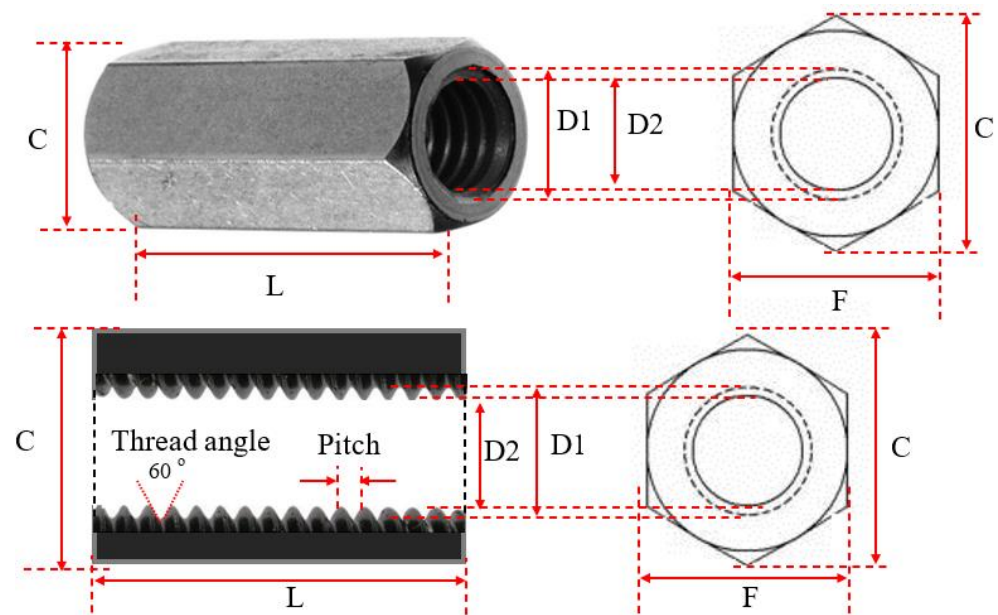**Figure 4.** Physical dimensions of structural bolts.

Figure 5. Physical dimensions of structural couplers.

2.3. Material Properties

The key material properties such as yield stress (f_y), ultimate stress (f_u), and elongation of structural bolts and couplers are presented in Tables 3 and 4. The yield stress ($f_{y,b}$) for M16, M20 and M24 bolts is 744 MPa, 737 MPa, and 714 MPa, respectively for 8.8 grade bolts, whereas 1017 MPa, 1022 MPa, and 981 MPa, respectively for 10.9 grade bolts. For the 5.6 and 8.8 grade couplers, the mean yield stress ($f_{y,c}$) is 300 MPa and 640 MPa, respectively. From the table, the yield stress and ultimate stress deepen on the bolts' size but remains constant for coupler size.

Table 3. Material properties of structural bolts.

Bolt Type	Bolt Grade	E_s (GPa)	$f_{y,b}$ (MPa)	$f_{u,b}$ (MPa)	Elongation (%)	Proof Load (kN)
M16-8.8	8.8	200	744	844	16.0	91
M16-10.9	10.9	200	1017	1091	12.7	130
M20-8.8	8.8	200	737	942	15.0	147
M20-10.9	10.9	200	1022	1084	12.9	203
M24-8.8	8.8	200	714	946	14.0	212
M24-10.9	10.9	200	981	1151	11.5	293

Table 4. Material properties of structural couplers.

Coupler Grade	E_s (GPa)	$f_{y,c}$ (MPa)	$f_{u,c}$ (MPa)
Grade 5.6	200	430	610
Grade 8.8	200	744	844

2.4. Test Set up and Testing Procedures

All bolt-coupler connection specimens were tested under compression using the 1000 kN capacity Universal Testing Machine (UTM). The specimens were placed on a rigid base plate of UTM, and the compressive loads were applied on top of the specimens directly using another rigid plate. A rigid plate was used to attain homogenous distribution of applied compressive load on the top of the specimens, as shown in Figure 6. To eliminate the gaps between the loading plate and specimens, a preload of 50 kN was applied before the actual load application. The load was applied in two steps using two different loading rates

under a displacement control method similar to the test conducted by Hassan et al. [32]. In the first step, the loading rate of 0.05 mm/min was considered and continued until an obvious inflection point, i.e., nearly yielding bolts. In the second step, the loading rate was increased to 0.3 mm/min until the bolt reached a significant deformation and failed. It is worth mentioning that bolt-coupler connection specimens are tested under compression, not under shear loading and load-axial deformation curves are measured only during testing.

Figure 6. Test setup for coupling bolts under pure axial compression.

3. Results and Discussion

3.1. Failure Modes of Bolt-Coupler Connections

The failure modes observed for eighteen tested bolt-coupler connection specimens are presented in Figures 7–9. These specimens are made with 8.8 and 10.9 grade M16, M20, and M24 fully threaded bolts with 8.8 grade couplers. Six specimens were tested with zero space between upper and lower bolts within the coupler (C-M16-8.8-0 and C-M16-10.9-0; C-M20-8.8-0 and C-M20-10.9-0; C-M24-8.8-0 and C-M24-10.9-0). It can be observed that the bolt-coupler connection failed due to the yielding of the upper bolt and the coupler did not experience any damage. When there was no gap between the upper and lower bolts, the compressive load applied on the top bolt is transferred by connecting the upper bolt to the lower bolt, which improves ultimate capacity. However, the failure mode of the remaining 12 bolt-coupler connections having a gap of 10 mm and 20 mm is different compared to the bolt-coupler connection with zero gaps. When there was a gap (10 mm or 20 mm) between upper and lower bolts, the applied load is transferred through the upper bolt to the coupler thread to the lower bolt. As a result, there was coupler thread failure, which stimulated the coupler outward buckling at the mid-height of the coupler especially for lower grade couplers (5.6 grade) compared to higher grade couplers (8.8 grade). In some cases, the upper and lower bolts are bent in opposite directions due to uneven coupler thread failure, as shown in Figure 9.

Figure 7. Failure modes of M16 bolts with 8.8 grade coupler. (**a**) M16-10.9 bolts. (**b**) M16-8.8 bolts.
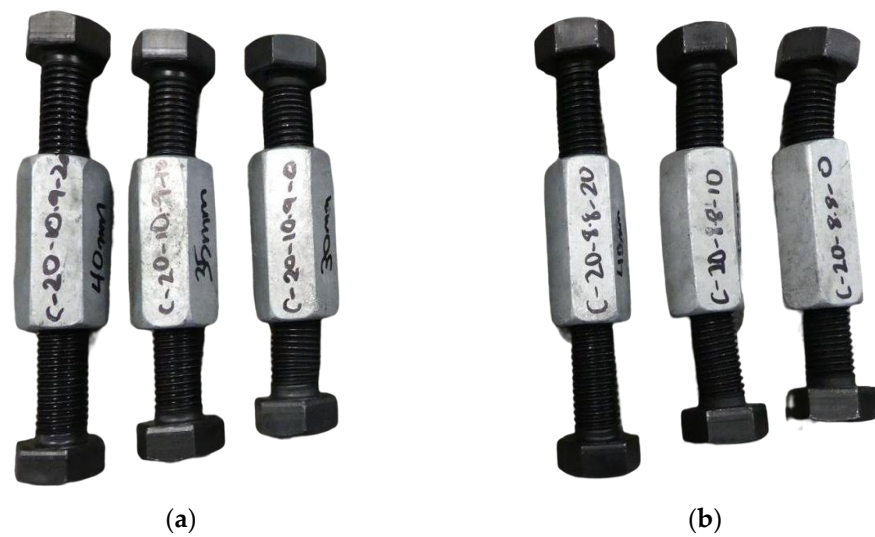

Figure 8. Failure modes of M20 bolts with 8.8 grade coupler. (**a**) M20-10.9 bolts, (**b**) M20-8.8 bolts.
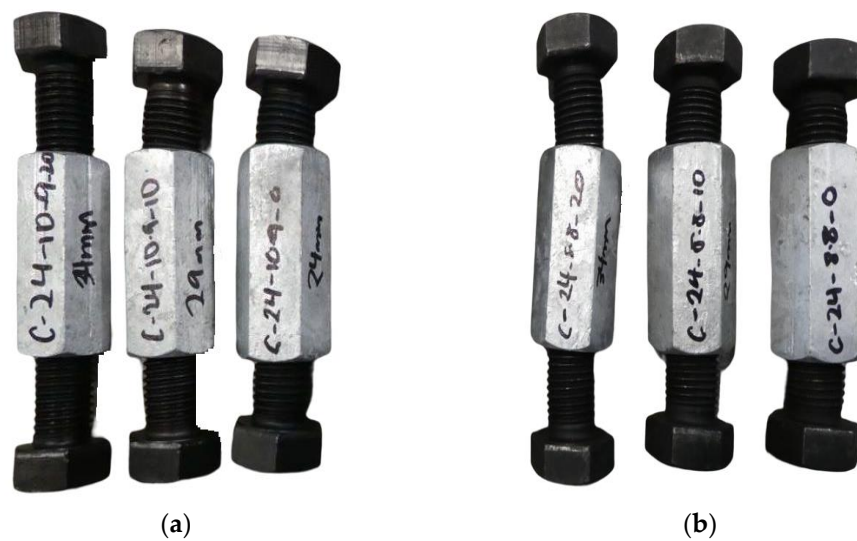

Figure 9. Failure modes of M24 bolts with 8.8 grade coupler. (**a**) M24-10.9 bolts, (**b**) M24-8.8 bolts.

3.2. Load-Deformation Curve of Bolt-Coupler Connections

The axial compression load-axial deformation curves of all tested bolt-coupler connection specimens are plotted in Figures 10–12. The load-axial deformation curves are compared for 8.8 and 10.9 grades structural bolts with different spacing gaps (0, 10, 20 mm). For all tested specimens, 8.8 grade structural couplers are used. The initial stiffness of the same bolt with different spacing gaps is observed almost the same. The load-axial deformation curves of each bolt-coupler connection having zero spacing gap are different than that of the bolt-coupler connections having 10 mm and 20 mm spacing gap. The strain hardening behaviour is observed more in the zero spacing bolt-coupler connections compared to the 10 mm spacing bolt-coupler connections. The ductility reduces with an increase in the spacing gap. The axial load-deformation curves are suddenly dropped after reaching the peak point and show brittle behaviour for a 20 mm spacing gap, as shown in Figures 10, 11 and 12a. For the higher strength grade bolts (10.9), similar trends on the load-deformation curves are observed, but ductility reduces fast compared to lower strength grade bolts, as shown in Figures 10, 11 and 12b. It can be seen from Figures 10–12 that the M24 bolts exhibit higher ductile behaviour compared to the M16 and M20 bolts. This could be due to the bolt threads and pitch value. As the load-axial deformation curves show strain hardening behaviour in most of the cases, the ultimate capacity (N_{ue}) was defined at the first peak where a strain-softening response is found. Otherwise, the load corresponding to 6 mm axial deformation is taken as the ultimate capacity. The N_{ue} values of 24 specimens tested under axial compression are summarised in Table 5.
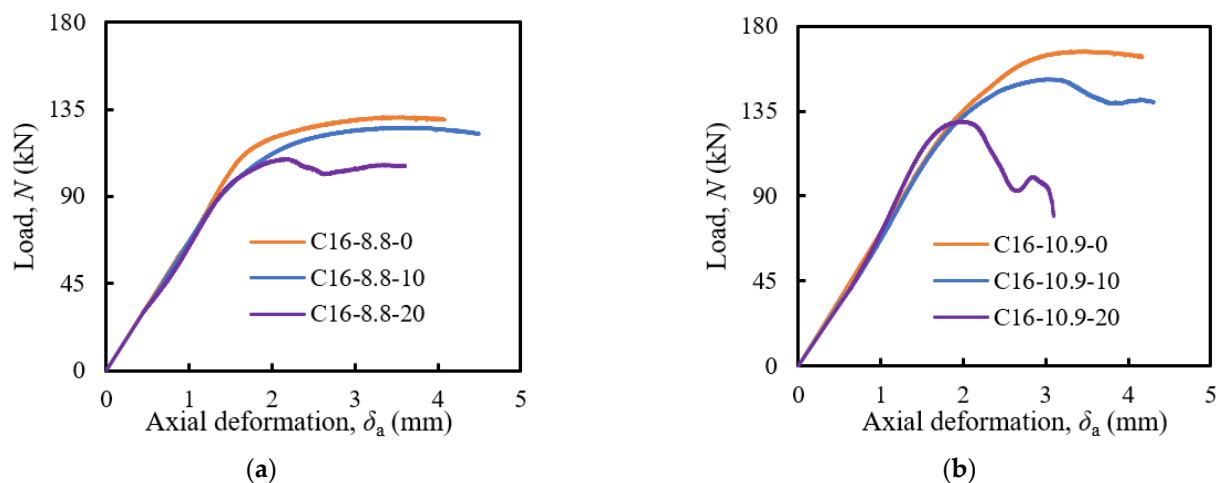

(**a**)

(**b**)

Figure 10. Compressive behaviour of M16 bolt-coupler connections. (**a**) 8.8 grade bolt and 8.8 grade coupler, (**b**) 10.9 grade bolt and 8.8 grade coupler.
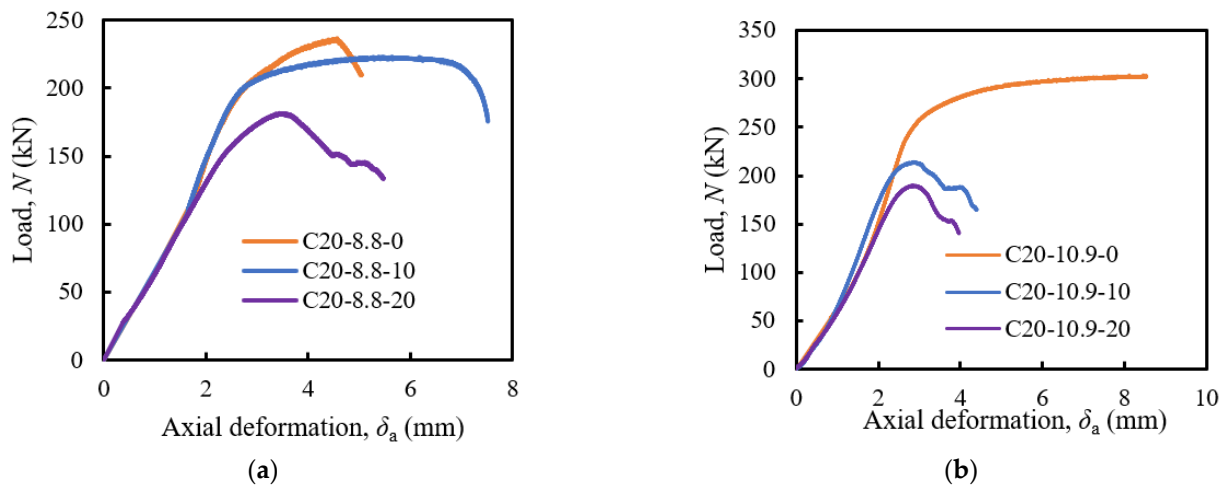
Figure 11. Compressive behaviour of M20 bolt-coupler connections. (**a**) 8.8 grade bolt and 8.8 grade coupler, (**b**) 10.9 grade bolt and 8.8 grade coupler.
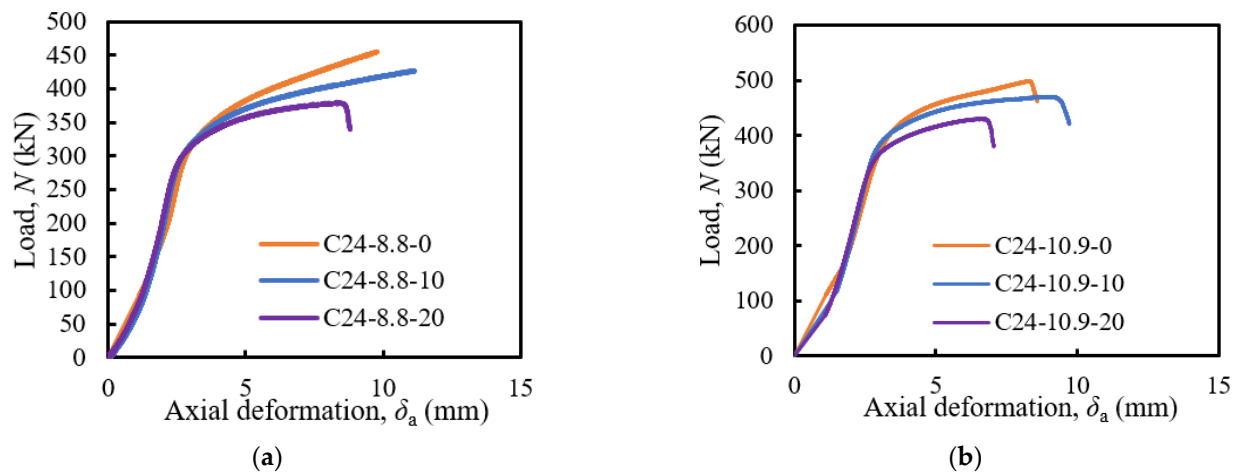

Figure 12. Compressive behaviour of M24 bolt-coupler connections. (**a**) 8.8 grade bolt and 8.8 grade coupler, (**b**) 10.9 grade bolt and 8.8 grade coupler.

Table 5. Strength capacity of tested specimens under compression at 6 mm axial deformation.

Test Number	Specimen Label	Bolt Size (mm)	Bolt Grade	Coupler Grade	Spacing (mm)	N_{ue} (kN)	N_{AS4100} (kN)	N_c (kN)
1	C-16-8.8-0	16	8.8	8.8	0	131.10	132.23	129.09
2	C-16-8.8-10	16	8.8	8.8	10	125.60	132.23	123.87
3	C-16-8.8-20	16	8.8	8.8	20	109.20	132.23	108.33
4	C-16-10.9-0	16	10.9	8.8	0	166.90	170.92	166.87
5	C-16-10.9-10	16	10.9	8.8	10	151.80	170.92	156.86
6	C-16-10.9-20	16	10.9	8.8	20	129.30	170.92	123.48
7	C-20-8.8-0	20	8.8	8.8	0	236.60	230.6	241.77
8	C-20-8.8-10	20	8.8	8.8	10	225.40	230.6	229.68
9	C-20-8.8-20	20	8.8	8.8	20	181.60	230.6	183.75
10	C-20-10.9-0	20	10.9	8.8	0	297.00	265.36	278.22
11	C-20-10.9-10	20	10.9	8.8	10	268.30	265.36	253.18
12	C-20-10.9-20	20	10.9	8.8	20	215.40	265.36	205.88
13	C-24-8.8-0	24	8.8	8.8	0	401.19	333.47	366.61
14	C-24-8.8-10	24	8.8	8.8	10	388.75	333.47	348.28
15	C-24-8.8-20	24	8.8	8.8	20	355.42	333.47	315.29
16	C-24-10.9-0	24	10.9	8.8	0	471.70	405.73	446.06
17	C-24-10.9-10	24	10.9	8.8	10	454.84	405.73	430.44
18	C-24-10.9-20	24	10.9	8.8	20	430.00	405.73	407.7
19	C-24-8.8-5.6-10	24	8.8	5.6	10	371.68	333.47	129.09
20	C-24-10.9-5.6-10	24	10.9	5.6	10	382.60	333.47	123.48

3.3. Discussion

3.3.1. Behaviour of Bolt-Bolt Connections with Coupler Compared to Single Bolts

The structural behaviour of single structural bolts without a coupler under compression was investigated experimentally and numerically in the previous paper [32]. The same structural bolts are used for making bolt-coupler connections and tested herein under axial compression. The test results of single structural bolts reported in a previous paper [32] are directly used in this study for comparison with the results of bolt-coupler connection with zero spacing gap. The comparison is presented for M16, M20, and M24 bolts with both 8.8 and 10.9 grade structural bolts in Table 6. For all cases, 8.8 coupler grade is used for bolt-coupler connection with zero spacing gap. As can be seen from Table 6, the ultimate capacity of the M16 single bolt is higher compared to the M16 bolt-coupler connection with zero spacing gap for both grades of the bolt. The load capacity of the M16 bolt-coupler connection with zero spacing gap is reduced by around 7% and 11.5% for 8.8 and 10.9 grade, respectively, compared to the M16 single bolts. A similar trend of results is also found for M20 bolts for 8.8 strength grade, whereas an opposite trend has been observed for 10.9 grade bolts. For M20-8.8 bolts, the percentage of load decrease is similar to the M16-8.8 bolts. However, the load capacity increases with the increase of bolt diameter of bolt-coupler connections for both grades compared to single bolts. This is because of the compression and bending effect observed in the upper and lower bolts of bolt-coupler connection, whereas single bolts are compressed and experienced energy imbalance due to unequal effective material in the tension zone and compression zone. This could be due to the less integrity in bolt-coupler connections with zero spacing gap compared to the single bolt.

**Table 6.** Comparison of strength capacity of single bolts and coupling bolts under compression.

Test Number	Specimen Label	Bolt Size (mm)	Bolt Grade	Coupler Grade	Spacing (mm)	N_{ue} (kN)
1	C-16-8.8-0	16	8.8	-	-	140.85
2	C-16-8.8-0	16	8.8	8.8	0	131.10
3	C-16-10.9-0	16	10.9	-	-	186.10
4	C-16-10.9-0	16	10.9	8.8	0	166.90
5	C-20-8.8-0	20	8.8	-	-	254.97
6	C-20-8.8-0	20	8.8	8.8	0	236.60
7	C-20-10.9-0	20	10.9	-	-	294.69
8	C-20-10.9-0	20	10.9	8.8	0	297.00
9	C-24-8.8-0	24	8.8	-	-	381.47
10	C-24-8.8-0	24	8.8	8.8	0	401.19
11	C-24-10.9-0	24	10.9	-	-	467.94
12	C-24-10.9-0	24	10.9	8.8	0	471.70

In this study, the integrity factor for bolt-coupler connection is determined. The integrity factor ($\gamma = \frac{N_{c,b-b}}{N_{c,b}}$) is defined as the ratio of ultimate capacity of bolt-coupler connections with zero spacing gap ($N_{c,b-b}$) and the capacity of a single bolt without a coupler ($N_{c,b}$). The γ value is determined from the measured data reported in Table 6 and plotted against the bolt size which is illustrated in Figure 13. It can be observed from this figure that the γ value increases with the increases in bolts size for both 8.8 and 10.9 grade bolts. The primary equation from the linear relationship of γ and bolt size is developed and expressed in Equation (1), which will be discussed in Section 4 and proposed more precisely for different bolt sizes used in the design equation in Section 4. The integrity factor (γ) is determined based on the current test data and used lower-bound to develop the equation of γ for safe prediction for all types of bolt grades.

$$\gamma = 0.43 + 4.1 \times 10^{-2}D - 7 \times 10^{-4}D^2 \tag{1}$$

where, D is the effective diameter of the bolt under compression, which can be determined using Equation (2) proposed in [32].

$$D = d_o - 0.58P \tag{2}$$
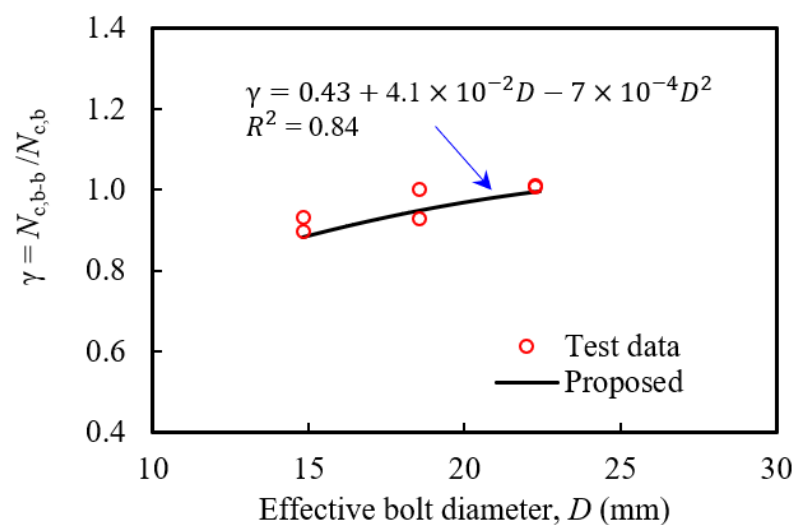
Figure 13. Integrity factor (γ) vs. effective bolt diameter.

3.3.2. Effect of Bolts Spacing Gap

The effect of the bolt spacing gap between upper and lower bolts is plotted in Figure 14 for M16, M20, and M24 bolt-coupler connections. The vertical axis represents the ultimate load ratio ($N_{u,s}/N_{u,0}$) where $N_{u,0}$ is the ultimate load capacity of bolt-coupler connections with zero spacing gap and $N_{u,s}$ is the ultimate load capacity of bolt-coupler connections with a 10 mm or 20 mm spacing gap. The ultimate load ratio changes with the spacing between upper and lower bolts inside the coupler. As can be seen, for both lower and higher-grade bolts, the capacity of bolt-coupler connections decreases with the increase of bolt spacing gaps. This is because of less thread interaction between bolt and coupler and thread failure trends of couplers significantly increased with the increases of bolt spacing gaps and specimens failed suddenly. However, the reduction of the ultimate ratio is higher for 10.9 grade bolts compared to 8.8 bolts for M16 bolt-coupler connections. A similar reduction ratio is almost observed for M20 bolt-coupler connections, as illustrated in Figure 14a,b. For the M24 bolt-coupler connection, the reduction of the ultimate capacity ratio is less compared to M16 and M20 bolt-coupler connections. There are no significant differences between lower and higher-grade bolts, as shown in Figure 14c. This might be due to the material property of the coupling bolt used in M24 bolt-coupler connections.
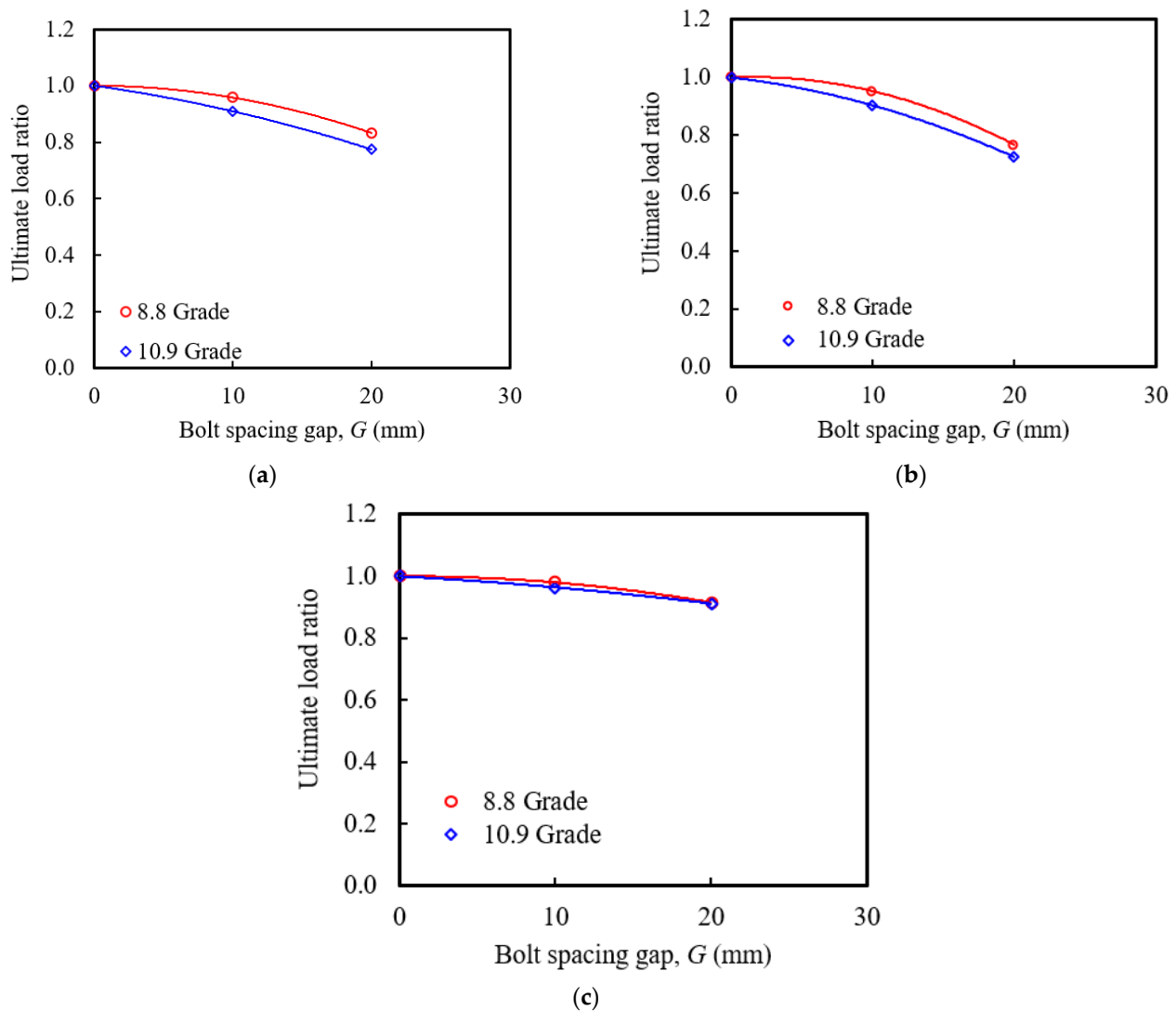

Figure 14. Effect of bolt spacing on compressive strength of PCC connections. (**a**) M16 bolt with 8.8 and 10.9 grade, (**b**) M20 bolt with 8.8 and 10.9 grade, (**c**) M24 bolt with 8.8 and 10.9 grade.

3.3.3. Effect of Bolt Diameters and Grades

The measured ultimate capacity of the tested specimens is shown in Figure 15a and the effect of bolts grades (8.8 and 10.9 grade) and bolt diameters (M16, M20, and M24 bolts) are illustrated in Figure 15b. It can be seen from the results for M16, M20, and M24 bolts with zero spacing that the ultimate capacity increase with the increase of the diameter of the bolts. This trend is similar for both bolts grades (8.8 and 10.9 grade bolts). The ultimate capacity of M16 bolts is 125.60 kN and 151.80 kN, respectively for 8.8 and 10.9 grade bolts. A load of M16 bolts with 10.9 grade and zero spacing increases by around 20.86% compared to the same bolt with an 8.8 grade bolt. For the M20 bolts, this percentage is slightly lower, and the value is 19.03%. On the other hand, the capacity increment of the 10.9 grade M24 bolt is 15.66% compared to the 8.8 grade M24 bolt which is 5.20% lower compared to M16 bolts. When the ultimate capacity of M20 and M24 bolts with the same grade is compared with M16 bolts, the ultimate capacity of M20 and M24 bolts increases by 1.79 and 3.13 times of the 8.8 grade M16 bolts, respectively. The capacity of 10.9 grade M20 and M24 bolts increases by 1.77 and 3.00 times the 10.9 grade M16 bolts, respectively. It can be concluded that the load capacity of the bolt increases with an increase in the bolt diameter with the same bolt grade and the bolt capacity of 10.9 grade bolts compared to 8.8 grade bolts decrease with an increase in the bolt diameter, as shown in Figure 15b.
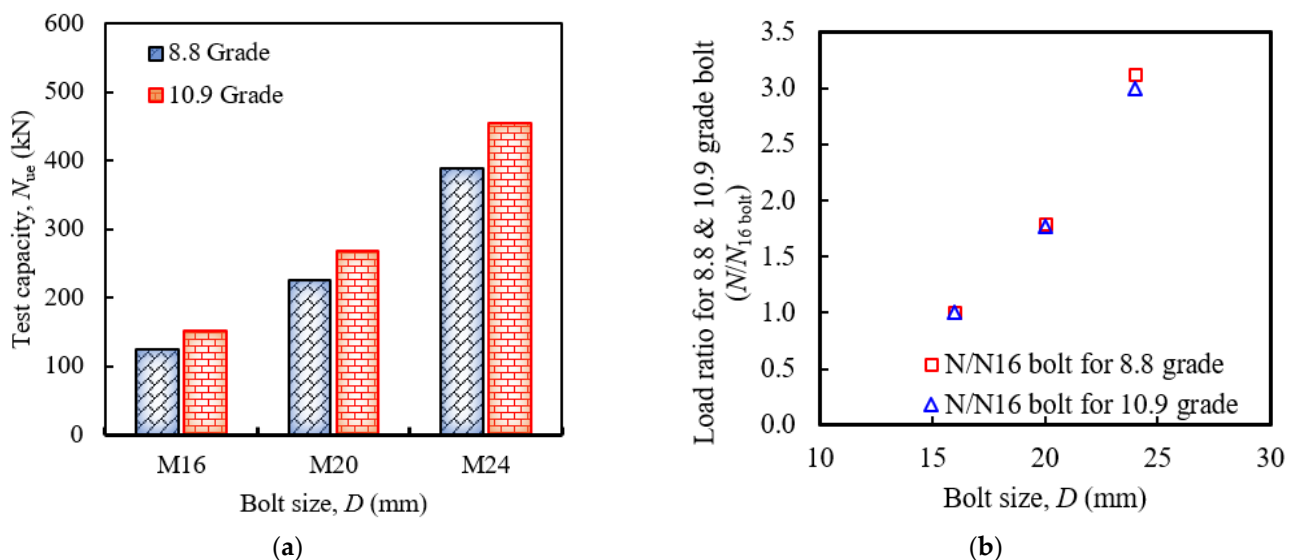

Figure 15. Effect of bolt grades on compressive strength of bolt-coupler connections. (**a**) Test capacity vs. bolt size, (**b**) Load ratio for 8.8 & 10.9 grade bolt ($N/N_{16\,bolt}$) vs. bolt size.

3.3.4. Effect of Coupler Grades

To investigate the effect of coupler grades (8.8 grade and 5.6 grade), M24 bolt-coupler connections with 8.8 and 10.9 grade bolts are tested. The test results are shown in Figure 16a for 8.8 grade M24 bolt-coupler connections and in Figure 16b for 10.9 grade M24 bolt-coupler connections. It can be seen from Figure 16a that the load capacity of M24 bolt-coupler connections with 8.8 grade coupler (C-24-8.8-10) is higher compared to the same bolt-coupler connections with 5.6 grade coupler (C-24-8.8-5.6-10). The load increment is more significant for 10.9 grade bolt-coupler connections, as shown in Figure 16b. The M24 bolt-coupler connections with 5.6 grade coupler (C-24-8.8-5.6-10 and C-24-10.9-5.6-10) are lower than that of M24 bolt-coupler connections with 8.8 grade coupler (C-24-8.8-10 and C-24-10.9-10). This is due to the failure of lower-grade couplers, as shown in Figure 17a,b. When 8.8 grade coupler is used in M24 bolt-coupler connections, the compression failure on the bolts is observed, and don't have any failure on the coupler. However, when a 5.6 grade coupler is used in M24 bolt-coupler connections, buckling failure on the coupler

is observed, and do not have any failure on the bolts. It indicates that the coupler has a significant influence on the ultimate capacity of bolt-coupler connections.
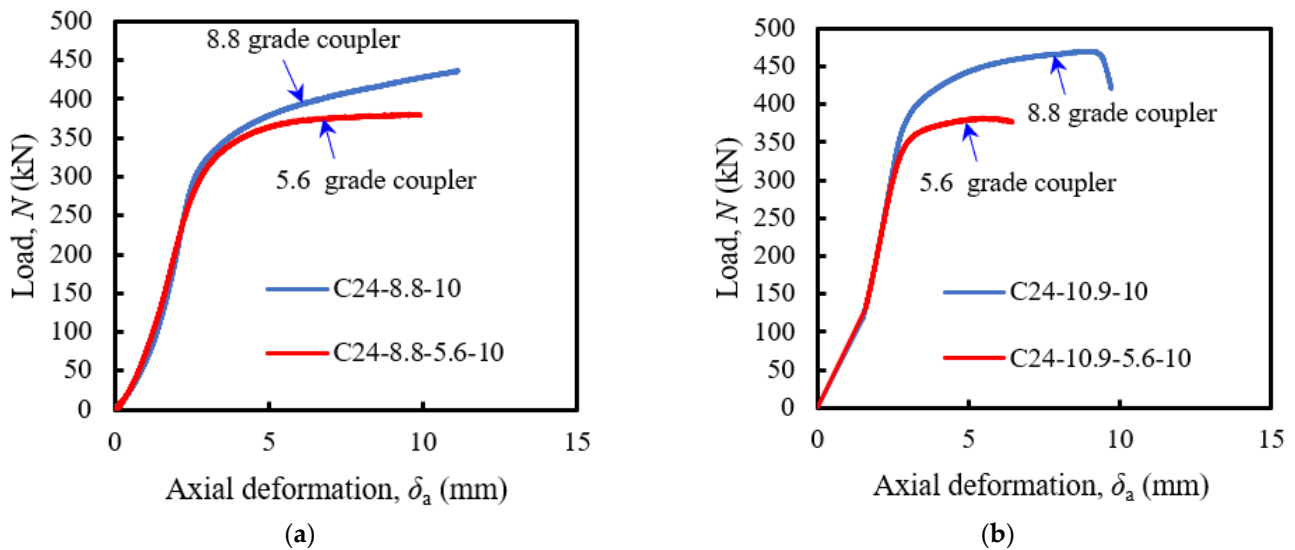

Figure 16. Effect of coupler grades on compressive strength of bolt-coupler connections. (**a**) M24 bolts with 8.8 grade bolts, (**b**) M24 bolts with 10.9 grade bolts.
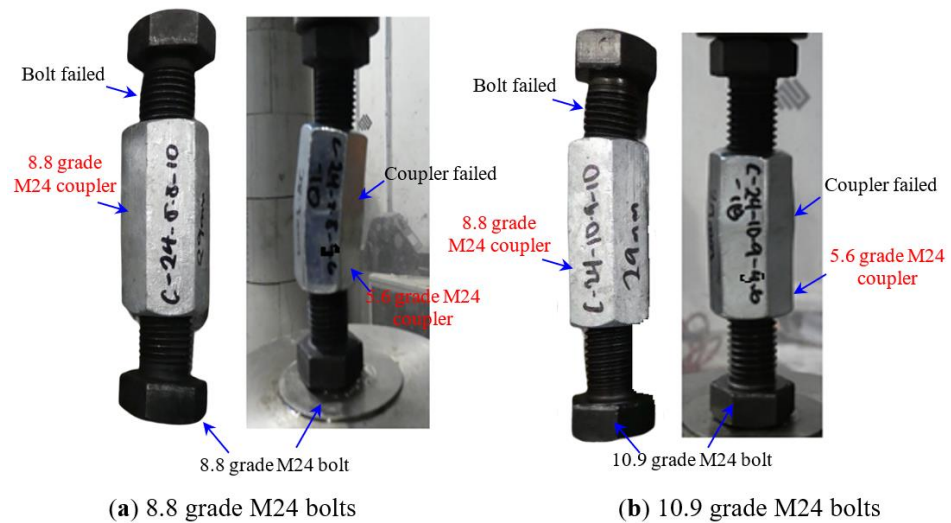

Figure 17. Failure modes of M24 bolts with 5.6 and 8.8 grade couplers.

4. Design Capacity of Bolt-Coupler Connections

4.1. Test Data Comparison with AS 4100

The existing code is developed for structural bolts under pure tension. According to the AS4100 code [33], the tensile capacity equation is expressed in Equation (3), where N_{AS4100} is the ultimate load capacity of bolts, $A_{s,b}$ is the effective cross-sectional area of the bolt, and $f_{u,b}$ is yield strength. Capacity reduction factor $\phi = 0.90$ was used to compute the design capacity (N^*_{AS4100}) of the bolt under tension as expressed in Equation (4).

$$N_{AS4100} = A_{s,b} f_{u,b} \tag{3}$$

$$N^*_{AS4100} \leq \phi N_{AS4100} \tag{4}$$

$$A_{s,b} = \frac{\pi}{4}(d_o - 0.9382P)^2 \tag{5}$$

The effective cross-sectional area ($A_{s,b}$) of structural bolts under pure tension lower compared to the nominal cross-sectional area of bolts. Necking is observed on the bolt when tested under tension and reduces the cross-sectional area. The reduced cross-sectional area is determined using Equation (5) recommended for bolts under tension, where P is the pitch of bolts. In this section, the capacity prediction by AS4100 (N_{AS4100}) is compared with the tested 20 bolt-coupler connection specimens (N_{ue}) and presented in Table 5. The mean value and the standard deviation are 1.024 and 0.146, respectively. It is worth noting that the predicted ultimate load capacity determined using Equation (3) based on the reduced cross-sectional area obtained from Equation (5) is very conservative for the bolt-coupler connections when the bolt spacing gap increases. It indicates that further modification is required to predict the strength capacity of bolt-coupler connections.

4.2. Design Recommendations

It revealed that an accurate design formula is crucial for bolt-coupler connections under pure compression. In the present study, the design equation (Equation (3)), used for bolts under tension, is modified and two additional parameters (γ and α) are introduced to accurately predict the ultimate strength capacity of bolt-coupler connections under compression. The revised design equation proposed for bolt-coupler connections under compression is expressed in Equation (6).

$$N_c = \gamma\alpha \times min \begin{cases} A_{s,\,b}f_{u,b} & \text{for bolt} \\ A_{s,c}f_{u,c} & \text{for coupler} \end{cases} \tag{6}$$

where $f_{u,b}$ is the tensile strength of the bolt, $f_{u,c}$ is the tensile strength of the coupler, $A_{s,b}$ is the effective cross-section area of the bolt and $A_{s,c}$ is the effective cross-section area of the coupler. The effective cross-section area of the bolt ($A_{s,b}$) and coupler ($A_{s,c}$) under compression can be calculated using Equation (7) proposed in [32] and using Equation (8), respectively.

$$A_{s,b} = \frac{\pi}{4}(d_o - 0.58P)^2 \tag{7}$$

$$A_{s,c} = \frac{\pi}{4}F^2 - A_{s,b} \tag{8}$$

The integrity factor (γ) is introduced in Equation (6) to consider the integrity effect of bolt-coupler connections as less integrity in bolt-coupler connections with zero spacing gap is observed compared to the single bolt. The integrity factor (γ) is determined using Equation (1) which is developed based on the test data discussed in Section 3.3.1. The bolt spacing gap factor (α) is introduced in Equation (6) to consider the effect of the bolt spacing gap (G) on the ultimate strength of bolt-coupler connections. The value of α is determined based on the ultimate load ratio of bolt-coupler connection with a spacing gap to bolt-coupler connection with zero spacing gap. The effect of the ultimate load ratio vs bolt spacing gap is illustrated in Figure 18 for different bolt sizes (M16, M20, and M24) and grades (8.8 and 10.9).
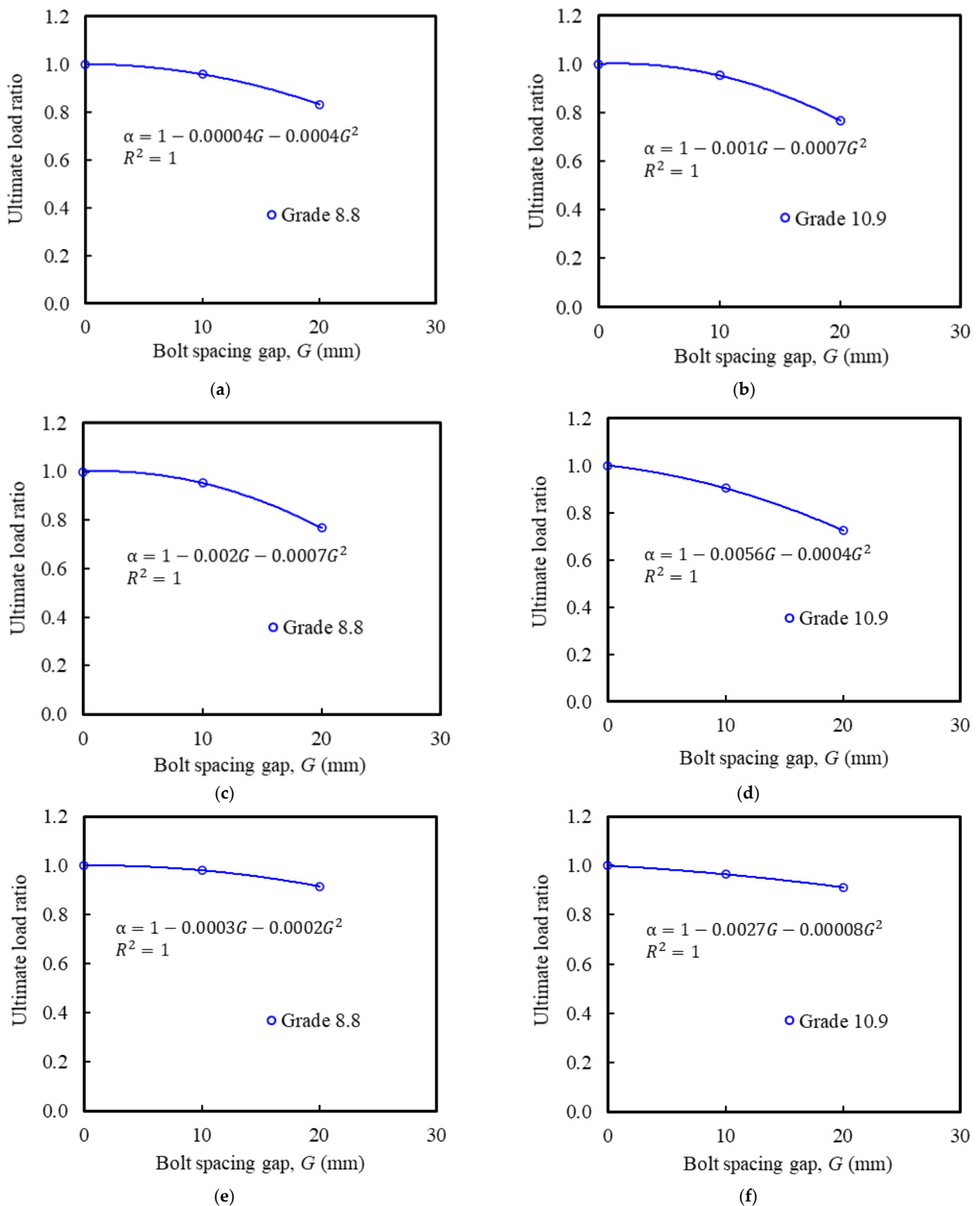
Figure 18. Strength reduction of bolt-coupler connections for different bolt spacing gaps. (**a**) M16 bolt with 8.8. (**b**) M16 bolt with 10.9 grade, (**c**) M20 bolt with 8.8, (**d**) M20 bolt with 10.9 grade, (**e**) M24 bolt with 8.8, (**f**) M24 bolt with 10.9 grade.

As the strength reduction (ultimate load ratio) of bolt-coupler connections for different bolt spacing gaps influences by bolt size and grade, a non-linear regression analysis has

been performed and proposed an equation for each bolt size and grade, which are presented in Equation (9) for 8.8 grade bolts and in Equation (10) for 10.9 grade bolts.

$$\alpha = \begin{cases} 1 - 0.00004G - 0.0004G^2 & \text{for } M16 \text{ bolts} \\ 1 + 0.002G - 0.0007G^2 & \text{for } M20 \text{ bolts} \\ 1 - 0.003G - 0.0002G^2 & \text{for } M24 \text{ bolts} \end{cases} \tag{9}$$

$$\alpha = \begin{cases} 1 + 0.001G - 0.0007G^2 & for\ M16\ bolts \\ 1 - 0.005G - 0.0004G^2 & for\ M20\ bolts \\ 1 - 0.0027G - 0.00008G^2 & for\ M24\ bolts \end{cases} \tag{10}$$

Based on the proposed equations of γ and α, the ultimate load capacity of all specimens of bolt-coupler connections is determined using Equation (6) and reported in Table 5. The predicted strength capacity of bolt-coupler connections is compared with the test results of all 20 tested specimens, as illustrated in Figure 19. It can be seen that the prediction capacity obtained from the proposed design equation (Equation (6)) is more accurate and safer for all cases. The mean value and the standard deviation are 0.966 and 0.046, respectively.
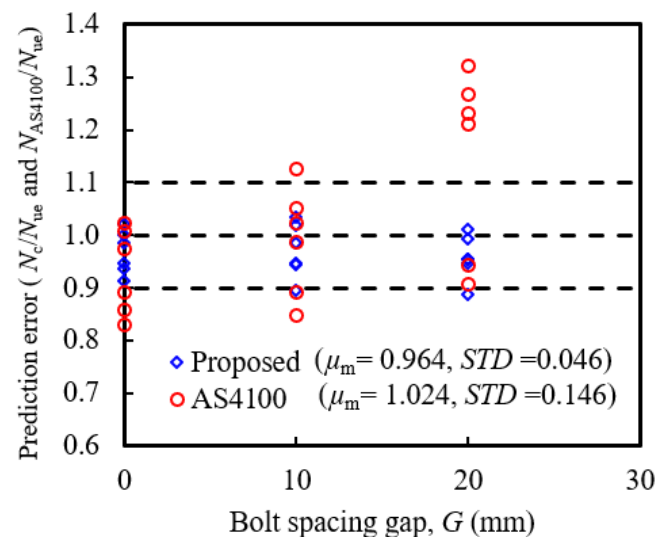

Figure 19. Comparison between the test, and proposed results.

5. Conclusions

The experimental investigation on bolt-coupler connections under compression has been conducted and considered around twenty-four specimens with different bolt sizes and grades. The failure modes, load-deformation curves, and ultimate load capacity are discussed. The main contribution of this study is to test the database and design equation development of bolt-coupler connections under compression which help to understand the compression behaviour and design of bolt-coupler connections for the construction of prefabricated CFST columns.

The following conclusions can be made based on the results reported in this paper.

(1) The failure modes of bolt-coupler connections mainly depend on the bolt spacing gaps and coupler strength. When the bolt spacing gap was zero, the failure of bolt-coupler connections with 8.8 grade bolts was due to the yielding of the upper bolt and the coupler did not experience any damage. When there was no gap between upper and lower bolts, there was coupler thread failure and yielding of the bolt.

(2) The coupler outward buckling was observed for the lower-grade couplers (5.6 grade) used in bolt-coupler connections. To avoid the coupler failure of bolt-coupler connections, 8.8 grade coupler should be sufficient when the bolt of 8.8 and 10.9 grade are in the bolt-coupler connections.

(3) The ultimate load capacity of bolt-coupler connections with zero spacing gap was observed lower compared to the single bolts tested under compression. This could be due to the less integrity in bolt-coupler connections with zero spacing gap compared to the single bolt.

(4) The ultimate load capacity of bolt-coupler connections with bolt spacing gap was reduced by increasing the bolt spacing gap. The maximum strength reduction was observed for 20 mm of bolt spacing gap and varied from 9–28% depending on the bolt sizes and grades.

(5) The predicted ultimate load capacity determined using existing design code AS4100 was very conservative for the bolt-coupler connections when the bolt spacing gap increases. The existing design equation is modified and introduced additional two parameters (γ and α) to predict accurately the ultimate strength capacity of bolt-coupler connections under compression. The prediction of ultimate load capacity obtained from the proposed design equation (Equation (6)) shows a better agreement with the test and gives a more accurate and safer prediction for all cases. The proposed design equation can be used by design engineers to determine the design capacity of bolt-coupler connections with a certain bolt spacing gap, which will give more confidence to the design of the prefabricated CFST columns with bolt-coupler connections.

Although experimental research on the bolt-coupler connection under compression (20 specimens) is conducted in this study, finite element analysis can be conducted to investigate the details behaviour of bolt-coupler connections under compression. In addition, repeatability tests, tests on bolt-coupler connections embedded in the concrete, and tests on bolt-coupler connections in prefabricated CFST columns can also be conducted before implementing the bolt-coupler connections in the construction of prefabricated CFST columns.

References

1. Mao, C.; Shen, Q.; Shen, L.; Tang, L. Comparative study of greenhouse gas emissions between off-site prefabrication and conventional construction methods: Two case studies of residential projects. *Energy Build.* **2013**, *6*, 165–176. [CrossRef]
2. Hassan, M.K.; Sheikh, M.N.; Saha, S. Behaviour, and design of prefabricated CFST stub columns with PCC connections under compression. *Thin Walled Struct.* **2021**, *166*, 108041. [CrossRef]
3. Zhang, X.; Skitmore, M.; Peng, Y. Exploring the challenges to industrialized residential building in China. *Habitat Int.* **2014**, *41*, 176–184. [CrossRef]
4. Hassan, M.K.; Tajhya, S. Numerical investigation of modified splice plate beam-to-beam connections for prefabricated composite structure. *Int. J. Eng. Constr. Comput.* **2019**, *1*, 27–35.
5. Jiang, Y.; Zhao, D.; Wang, D.; Xing, Y. Sustainable performance of buildings through modular refabrication in the construction phase: A comparative study. *Sustainability* **2019**, *11*, 5658. [CrossRef]
6. Hassan, M.K.; Subramanian, K.B.; Saha, S.; Sheikh, M.N. Behaviour of prefabricated steel-concrete composite slabs with a novel interlocking system-Numerical analysis. *Eng. Struct.* **2021**, *245*, 112905. [CrossRef]

7. Han, L.H.; Bjorhovde, R.; Li, W. Developments, and advanced applications of concrete-filled steel tubular (CFST) structures: Members. *J. Constr. Steel Res.* **2014**, *100*, 211–228. [CrossRef]

8. Liu, Y.; Ma, H.; Li, Z.; Wang, W. Seismic behaviour of full-scale prefabricated RC beam-CFST column joints connected by reinforcement coupling sleeves. *Structures* **2020**, *28*, 2760–2771. [CrossRef]

9. Uy, B. Strength of short concrete filled high strength steel box columns. *J. Constr. Steel Res.* **2001**, *57*, 113–134. [CrossRef]

10. Sakino, K.; Nakahara, H.; Morino, S.; Nishiyama, I. Behaviour of centrally loaded concrete-filled steel-tube short columns. *J. Struct. Eng.* **2004**, *130*, 180–188. [CrossRef]

11. Shim, C.S.; Kim, J.H.; Chung, C.H.; Chang, S.P. The behaviour of shear connection in a composite beam with full-depth precast slab. *Proc. Inst. Civ. Eng—Struct. Build.* **2000**, *140*, 101–110. [CrossRef]

12. Ataei, A.; Bradford, M.A.; Valipour, H.R. Experimental study of flush end plate beam-to-CFST column composite joints with deconstructable bolted shear connectors. *Eng. Struct.* **2015**, *99*, 616–630. [CrossRef]

13. Lam, D.; Dai, X.; Ashour, A.; Rehman, N. Recent research on composite beams with demountable shear connectors. *Steel Constr.* **2017**, *10*, 125–134. [CrossRef]

14. Uy, B.; Patel, V.; Li, D.; Aslani, F. Behaviour, and design of connections for demountable steel and composite structures. *Structures* **2017**, *9*, 1–12. [CrossRef]

15. Li, D.; Uy, B.; Patel, V.; Aslani, F. Behaviour, and design of demountable CFST column-column connections subjected to compression. *J. Constr. Steel Res.* **2018**, *141*, 262–274. [CrossRef]

16. Yang, F.; Liu, Y.; Jiang, Z.; Xin, H. Shear performance of a novel demountable steel concrete bolted connector under static pushout tests. *Eng. Struct.* **2018**, *160*, 133–146. [CrossRef]

17. Qing, Y.; Wang, C.L.; Meng, S.; Zeng, B. Experimental study on the seismic performance of precast concrete columns with thread-bolt combination couplers. *Eng. Struct.* **2022**, *251*, 113461. [CrossRef]

18. Kumar, R.; Mandal, P.K.; Narayan, A.; Das, A.J. Evaluation of load transfer mechanism under axial loads in a novel coupler of dual height rock bolts. *Int. J. Min. Sci. Technol.* **2021**, *31*, 225–232. [CrossRef]

19. Kwon, G.; Engelhardt, M.D.; Klingner, R.E. Experimental behaviour of bridge beams retrofitted with post installed shear connectors. *J. Bridge Eng.* **2011**, *16*, 536–545. [CrossRef]

20. Xue, W.; Bai, H.; Dai, L.; Hu, X.; Dubec, M. Seismic behaviour of precast concrete beam-column connections with bolt connectors in columns. *Struct. Concr.* **2020**, *22*, 1297–1314. [CrossRef]

21. Pitrakkos, T.; Tizani, W.; Cabrera, M.; Salh, N.F. Blind bolts with headed anchors under combined tension and shear. *J. Constr. Steel Res.* **2021**, *179*, 106546. [CrossRef]

22. Song, Y.; Wang, J.; Uy, B.; Li, D. Experimental behaviour, and fracture prediction of austenitic stainless-steel bolts under combined tension and shear. *J. Constr. Steel Res.* **2020**, *166*, 105916. [CrossRef]

23. Nijgh, M.P.; Gîrbacea, I.A.; Veljkovic, M. Elastic behaviour of a tapered steel-concrete composite beam optimized for reuse. *Eng. Struct.* **2019**, *183*, 366–374. [CrossRef]

24. Xue, W.; Yang, X.; Hu, X. Full-scale tests of precast concrete beam-column connections with composite T-beams and cast in-place columns subjected to cyclic loading. *Struct. Concr.* **2019**, *21*, 169–183. [CrossRef]

25. Ataei, A.; Bradford, M.A.; Liu, X. Experimental study of composite beams having a precast geopolymer concrete slab and deconstructable bolted shear connectors. *Eng. Struct.* **2016**, *114*, 1–13. [CrossRef]

26. *EN 1994-1-1*; Eurocode 4: Design of Composite Steel and Concrete Structures, Part 1-1: General Rules and Rules for Buildings. European Standard: London, UK, 2004.

27. Yang, F.; Liu, Y.; Xin, H.; Veljkovic, M. Fracture simulation of a demountable steel concrete bolted connector in push-out tests. *Eng. Struct.* **2021**, *239*, 112305. [CrossRef]

28. Ding, B.; Zhao, Y.; Huang, Z.; Cai, L.; Wang, N. Tensile bearing capacity for bolted spherical joints with different screwing depths of high-strength bolts. *Eng. Struct.* **2020**, *225*, 111255. [CrossRef]

29. Zhang, Y.; Chen, B.; Liu, A.; Pi, Y.L.; Zhang, J.; Wang, Y.; Zhong, L. Experimental study on shear behaviour of high strength bolt connection in prefabricated steel-concrete composite beam. *Compos. Part B* **2019**, *159*, 481–489. [CrossRef]

30. Wang, W.; Zhang, X.D.; Zhou, X.L.; Zhang, B.; Chen, J.; Li, C. Experimental study on shear performance of an advanced bolted connection in steel-concrete composite beams. *Case Stud. Constr. Mater.* **2022**, *16*, e01037. [CrossRef]

31. Lee, S.W.; Nestler, A. Simulation-aided design of Thread Milling Cutter. In Proceedings of the 5th CIRP Conference on High Performance Cutting, Zurich, Switzerland, 4–7 June 2012; pp. 120–125.

32. Hassan, M.K.; Ahmed, B.; Saha, S. Effect of bolt thread on the failure mode and ultimate capacity of bolts under tension and compression. In Proceedings of the 3rd International Conference on Structural Engineering Research, Sydney, Australia, 27–30 November 2022.

33. *AS 4100 1998*; Steel Structures. Standards Australia: Sydney, Australia, 2016.